Self-assembly of fibronectin into fibrillar networks underneath dipalmitoyl phosphatidylcholine monolayers: Role of lipid matrix and tensile forces

Gretchen Baneyx and Viola Vogel*

Department of Bioengineering, University of Washington, Seattle, WA 98195

Edited by John A. Glomset, University of Washington, Seattle, WA, and approved August 18, 1999 (received for review April 29, 1999)

The cell-mediated assembly of fibronectin (Fn) into fibrillar matrices is a complex multistep process that is incompletely understood because of the chemical complexity of the extracellular matrix and a lack of experimental control over molecular interactions and dynamic events. We have identified conditions under which Fn assembles into extended fibrillar networks after adsorption to a dipalmitoyl phosphatidylcholine (DPPC) monolayer in contact with physiological buffer. We propose a sequential model for the Fn assembly pathway, which involves the orientation of Fn underneath the lipid monolayer by insertion into the liquid expanded (LE) phase of DPPC. Attractive interactions between these surface-anchored proteins and the liquid condensed (LC) domains leads to Fn enrichment at domain edges. Spontaneous self-assembly into fibrillar networks, however, occurs only after expansion of the DPPC monolayer from the LC phase though the LC/LE phase coexistence. Upon monolayer expansion, the domain boundaries move apart while attractive interactions among Fn molecules and between Fn and domain edges produce a tensile force on the proteins that initiates fibril assembly. The resulting fibrils have been characterized *in situ* by using fluorescence and light-scattering microscopy. We have found striking similarities between fibrils produced under DPPC monolayers and those found on cellular surfaces, including their assembly pathways.

Fibronectin (Fn) is a multifunctional glycoprotein that exists in body fluids as a compact 440- to 500-kDa dimer and is assembled by cells into insoluble fibrillar networks. The protein is found in a fibrillar state in the extracellular matrix, basement membranes, and connective tissues. This form of Fn mediates most of the molecule's known biological functions, including the guiding of cell migration during wound healing and embryogenesis (1).

The cell-mediated assembly of soluble Fn into fibrillar matrices is a complex multistep process that is initiated only after cells adhere to surfaces. The first step in *de novo* fibril assembly involves a reversible interaction of the protein with the cell surface (2, 3). Binding to activated integrins in focal adhesions and subsequent self-association triggers the irreversible aggregation of Fn into large detergent-insoluble fibrillar matrices (4–8). Although the precise structure of the fibrils is unknown, they are elastic (9), and individual proteins appear to be assembled into periodic arrays in an extended conformation (10, 11).

While cell-based studies with recombinant Fn and peptide fragments have helped identify Fn modules that are essential for matrix assembly (3, 7, 12), little is known regarding the molecular pathway by which Fn is transformed into the fibrillar state. Complicating factors include the existence of multiple recognition sites for other extracellular matrix and transmembrane proteins, as well as the ability of Fn to anchor at interfaces by means of hydrophobic and electrostatic interactions. The complexity of these interactions combined with a lack of control over other dynamic events that accompany cell adhesion makes a detailed analysis of the Fn fibril assembly pathway difficult when cell-based assays are used.

Several cell-free routes have been identified that induce Fn fibril formation, including the addition of denaturants (13), reducing agents (14, 15), or peptidic fragments of the purified protein (4, 16). Fiber formation can also be induced by shear stress in the absence of additives (17, 18). The resulting fibrils exhibit the high molecular weight characteristic of the cell-mediated fibrillar networks. However, whether their structure or assembly mechanism is equivalent to that of cellular matrices remains unclear. Moreover, such systems allow little control over assembly parameters and do not permit the investigation of sequential events.

Our goal was to identify conditions under which Fn fibril assembly can be induced at membrane-mimetic surfaces in contact with physiological buffer. Fn was therefore adsorbed to receptor-free membrane-mimetic interfaces, prepared by spreading dipalmitoyl phosphatidylcholine (DPPC) monolayers at the air/buffer interface in a Langmuir trough. DPPC was chosen as a model interface for two reasons. On the biological side, the major lipid fraction in the outer leaflet of most cell membranes, including erythrocytes, and the apical plasma membrane of aortic endothelial cells contains phosphatidylcholine headgroups. On the physicochemical side, DPPC can exist at the air/water interface in three different two-dimensional phases at room temperature: a highly expanded "gas" phase, an intermediate fluid [the liquid expanded (LE) phase] and a densely packed phase [the liquid condensed (LC) phase]. The physical state and thus the molecular packing of DPPC lipid monolayers can be easily controlled by the use of movable barriers. Upon compression, the monolayer passes through a reversible first-order phase transition in which LC domains coexist with the LE phase. In this paper we show that Fn can spontaneously self-assemble into fibrillar networks underneath DPPC monolayers when the monolayer is gradually expanded from the LC phase, through the phase coexistence, and into the LE state. The resulting microscopic protein fibrils were characterized by fluorescence and light-scattering microscopy (LSM). A sequential model for Fn self-assembly underneath DPPC monolayers is proposed, and its relevance to Fn fibril formation in biological systems is discussed. The utility of the model system for investigating the assembly pathway and physical properties of Fn fibrils is also described.

Materials and Methods

Material. Human plasma Fn (>95% purity) was obtained from GIBCO Life Technologies, and albumin and fibrinogen were purchased from Sigma. DPPC (L isomer) and 1-palmitoyl

This paper was submitted directly (Track II) to the PNAS office.

Abbreviations: Fn, fibronectin; DPPC, dipalmitoyl phosphatidylcholine; LC, liquid condensed; LE, liquid expanded; LSM, light-scattering microscopy; POPC, 1-palmitoyl 2-oleoyl phosphatidylcholine; TRITC, tetramethylrhodamine isothiocyanate.

*To whom reprint requests should be addressed. E-mail: vvogel@u.washington.edu.

The publication costs of this article were defrayed in part by page charge payment. This article must therefore be hereby marked "*advertisement*" in accordance with 18 U.S.C. §1734 solely to indicate this fact.

2-oleoyl phosphatidylcholine (POPC) were purchased from Avanti Polar Lipids and used without further purification. Water from a Barnstead Millipore system was used, delivering 18-MΩ resistivity.

Protein Labeling and Labeling Stoichiometry. Tetramethylrhodamine isothiocyanate (TRITC) was obtained from Molecular Probes. TRITC labeling was performed according to standard protocols (Molecular Probes). Labeling stoichiometry was determined by the method of Haugland (19). The typical labeling ratio for Fn was 4.1 ± 0.4 fluorophores per protein molecule ($n = 3$). Proteins were used immediately. Buffer (10 mM Hepes/150 mM NaCl/1.5 mM $CaCl_2$, pH 7.4) was prepared according to Frey *et al*. (42). Surface pressure–area isotherms at the air/buffer interface were measured in a Langmuir trough with both labeled and unlabeled proteins to test whether the fluorescent label caused alterations in interfacial behavior. No change in surface behavior was observed (data not shown).

Preparation of Monolayers. Pure lipid monolayers were prepared at the air/water and air/buffer interface in a Teflon trough (8 × 18 × 0.7 cm) at 22 ± 1°C and monitored by using the Wilhelmy plate technique (20). The trough and barriers were cleaned with RBS (Pierce), and rinsed three times by sonication for 20 min in Nanopure water. Stock solutions of individual lipids (≈1 mg/ml) were prepared in chloroform. Approximately 15 nmol of lipid was spread at the interface and compressed between the two barriers at speeds not exceeding 0.4 $Å^2$ per molecule per min. Film balance measurements and barrier movements were controlled through a customized Labview 2 interface (National Instruments, Austin, TX) using a personal computer.

Protein Adsorption. After compression of the lipid monolayer, Fn was injected into the buffer subphase along the outside of the Teflon barriers (21), equilibrating at a final concentration of 4 μg/ml.

Fluorescence Microscopy of Monolayers. Surface-adsorbed proteins were visualized by using a Nikon custom-built epifluorescence microscope with *x*–*y* positioning mounted over a Langmuir trough. The microscope was equipped with a 40× long-working-distance objective (Nikon) and a charge-coupled device camera (Pulnix, Sunnyvale, CA) with intensifier (Intevac, Palo Alto, CA). Fluorescence excitation was with a high-pressure Hg lamp (100 W) and a rhodamine filter cube (DM580, Nikon). Images were captured digitally with National Institutes of Health IMAGE software.

LSM. A light-scattering microscope was built in our laboratory that can image the light scattered from nanoscale particles. For this application, a 10-mW He/Ne 632-nm laser beam strikes the air/water interface at an angle of 53° relative to the interface normal. Light scattered normal to the surface plane is collected by the same objective and detection system used for fluorescence microscopy. This system can readily detect latex spheres (refractive index $n = 1.4$) with diameters of 100 nm or greater (43). Fluorescence and light-scattering signals are distinguished by the use of proper filter combinations so that fluorescence images do not contain traces of scattered light and vice versa. Fluorescence and light-scattering images were taken ≈10 s apart. Because of convection-driven lateral monolayer movement, they do not represent identical regions of the interface.

Fluorescence Quenching with Iodine. Fluorescence quenching of TRITC by potassium iodide (KI) was first tested in solution in a Hitachi F-4500 fluorescence spectrophotometer by using experimental Fn concentrations (4 μg/ml). An optimal concentration of 0.3 M KI caused total loss of fluorescence within 30 min.

SDS/PAGE of Interfacial Proteins. Proteins at the air/buffer interface were gently pipetted from the surface and separated from lipids by extraction with chloroform/methanol (22). Reducing and nonreducing SDS/PAGE was performed on 9% resolving gels with 4% stackers, and proteins were visualized by silver staining.

Results and Discussion

Fn Adsorption to DPPC in the LE Phase and LE/LC Phase Coexistence. The influence of the physical state of the lipid monolayer on the adsorption behavior of Fn was investigated with DPPC. First, DPPC was spread on physiologic buffer and compressed into the LE phase to a surface pressure (π) of 2 mN/m and mean molecular area of 85 $Å^2$ per DPPC molecule. After 30-min equilibration at constant area, TRITC-labeled Fn was injected underneath the barriers into the subphase (final concentration 4 μg/ml). Within minutes, a rapid rise in surface pressure was observed, suggesting partial insertion of Fn into the interface. However, no obvious microscopic features were visible until the Fn concentration became high enough to induce the LE/LC phase transition in the lipid monolayer ($\pi \approx 7$ mN/m). At this point Fn was observed around the edges of small circular lipid LC domains (Fig. 1*a*). As the surface pressure rose, the fluorescence intensity in the LE phase increased and smaller LC domains (≈1-μm diameter) nucleated between the original LC domains (Fig. 1*b*). Although the surface pressure continued to increase to a final value of 10 mN/m in 3 h, there was no further change in monolayer appearance beyond that depicted in Fig. 1*c*, and light scattering remained at background levels.

The above experiment was repeated with a DPPC monolayer

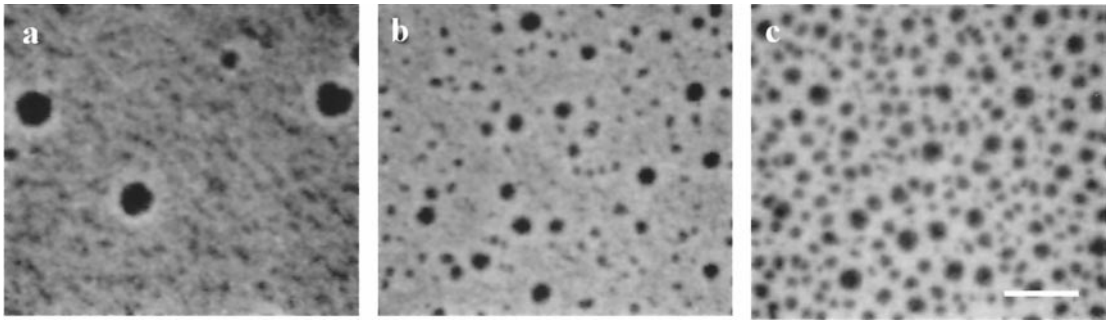

Fig. 1. Fn adsorbed to a DPPC monolayer in the LE phase. Fluorescence images were taken at 30 min and 7.1 mN/m (*a*) 40 min and 8.0 mN/m (*b*), and 180 min and 11.0 mN/m (*c*). TRITC-labeled Fn is initially concentrated at the edges of round DPPC domains. As the protein continues to adsorb, an increasing number of small domains appear and Fn homogeneously distributes around them. (Scale bar is 10 μm.)

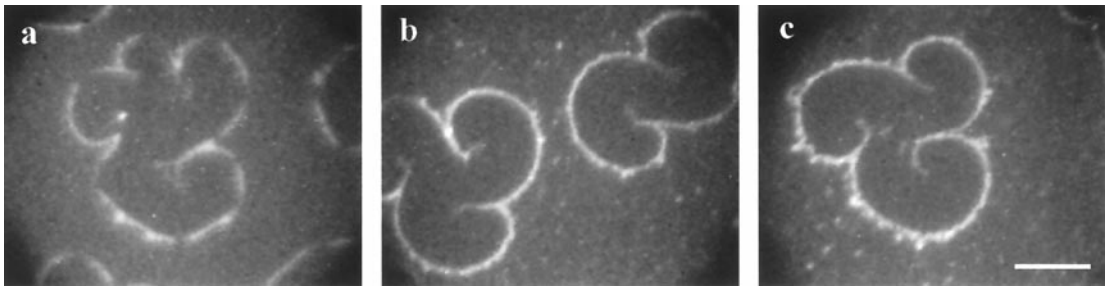

Fig. 2. Fn adsorbed to a DPPC monolayer in the LE/LC phase coexistence. Fluorescence images were taken at 60 min and 7.9 mN/m (*a*), 70 min and 9.2 mN/m (*b*) and 75 min and 9.5 mN/m (*c*). After 60 min, dark LC domains are surrounded by a lighter LE phase; brightly fluorescent rims of Fn can be seen at domain edges. DPPC domains have the characteristic triskelion shape reported for chiral DPPC in phase coexistence (41). Over time, fluorescent Fn aggregates appear in the LE phase and collect around the domains (*c*). (Scale bar is 20 μm.)

that had been compressed into the LE/LC phase coexistence region (π = 5 mN, 65 Å^2 per molecule). Approximately 1 h after injection, TRITC-labeled protein was observed at the interface as faint patches localized around chiral DPPC domains (Fig. 2*a*). As the Fn density in the interface increased, bright rims of Fn surrounded the domains and small fluorescent patches (1 to 2 μm in diameter) appeared in the LE phase (Fig. 2*b*). These patches grew, eventually becoming attracted to the domain edges (Fig. 2*c*). Unlike the previous experiment, only a small increase in interfacial π was observed ($\approx$3 mN/m).

Taken together, the above results indicate that Fn preferentially inserts into LE phase regions and that it does not bind to DPPC in the LC phase. Our data also suggest a limited solubility of Fn in the LE phase of DPPC: as it exceeds a critical density, single Fn molecules that appear homogeneously distributed in the LE phase coexist with an aggregated state visible in fluorescence as bright spots. Because these aggregates do not give rise to detectable light scattering, they are likely to be two-dimensional. It is significant for the interpretation of later results that Fn and Fn aggregates accumulate around DPPC domain edges. This accumulation at domain edges implies that attractive forces are acting between Fn in the LE phase and the domains. The insertion of proteins into the LE phase and migration to domain boundaries is not unique to Fn and has been observed for several other proteins (21, 23–25). Two nonexclusive theoretical models have been proposed to account for the attractive interaction between domain boundaries and surface-adsorbed proteins in the LE phase: attractive dipole/dipole interactions (26) and entropy-driven depletion forces (27). These are general mechanisms for protein interaction with lipid monolayers, and they presumably define the first step in the sequential pathway of fibril assembly.

Fn Assembles into Fibrillar Networks Only After Monolayer Expansion. Spontaneous assembly of Fn into fibrillar networks was observed when TRITC-labeled Fn was adsorbed underneath a DPPC monolayer that was subsequently expanded. Fig. 3 shows the surface pressure/area isotherm: representative fluorescence and light-scattering microscope images are presented in Fig. 4. The DPPC monolayer was first compressed on physiological buffer into the LC phase (π = 25 mN/m, 45 Å^2 per DPPC molecule). Fn was then injected into the subphase (final concentration 4 μg/ml) and allowed to equilibrate at constant area for 15 h. During this period, π remained essentially constant and no increase in fluorescence intensity was observed, confirming that Fn does not adhere to DPPC in the LC phase. Next, the monolayer was slowly expanded at speeds ranging between 0.14 and 0.4 Å^2 per molecule per min. Fn first binds to the interface surrounding the nonfluorescent LC domains at π = 16 $\pm$ 1 mN/m and an area of 50 $\pm$ 2 Å^2 per DPPC molecule (Fig. 4*a*). Interestingly, pure DPPC is still in the LC phase at this molecular area.

After $\approx$1 h of expansion (from 45 to 65 Å^2 per DPPC molecule), a second population of Fn became visible as fiber-like gray structures extending from the edges of dark lipid LC domains (Fig. 4*b*). Concurrent LSM revealed that these darker structures gave rise to strong light scattering, whereas the light-scattering intensity from the LC phase and the protein-rich LE phase remained below the detection limit of our system. The first fibrils were barely thick enough to be resolved in the fluorescence microscope. However, they grew thicker with continued expansion ($\approx$5 to 15 μm) and became interconnected as the lipid domains melted (Fig. 4*c*). The intensity of light scattering increased as the individual strands grew thicker (Fig. 4 *e–h*) and was independent of both the polarization and direction of the incoming light. Control experiments using unlabeled Fn resulted in identical light-scattering behavior, demonstrating that fibril formation was not an artifact caused by the labeling process.

Once formed, the networks remained irreversibly adsorbed to the interface, appearing increasingly fractal in the absence of lipid domains at high surface areas (Fig. 4*d*). Fibrils were stable

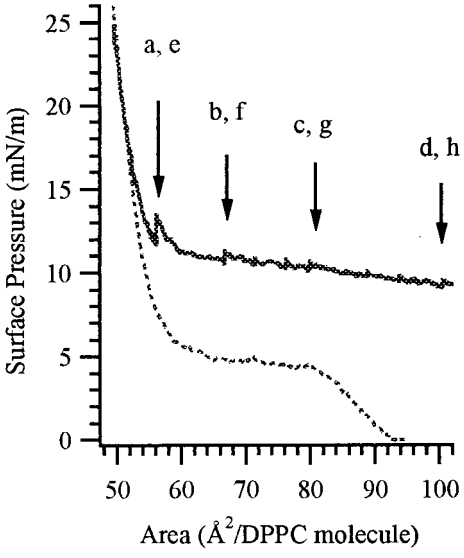

Fig. 3. Surface pressure/area isotherms. The dotted line shows the compression isotherm for pure DPPC on a plain air/buffer subphase; the solid line shows the expansion isotherm after Fn injection and equilibration for 15 h (pH 7.4, ionic strength 0.2 M, 22°C). Arrows indicate the points on the isotherm at which the images in Fig. 4 were taken.

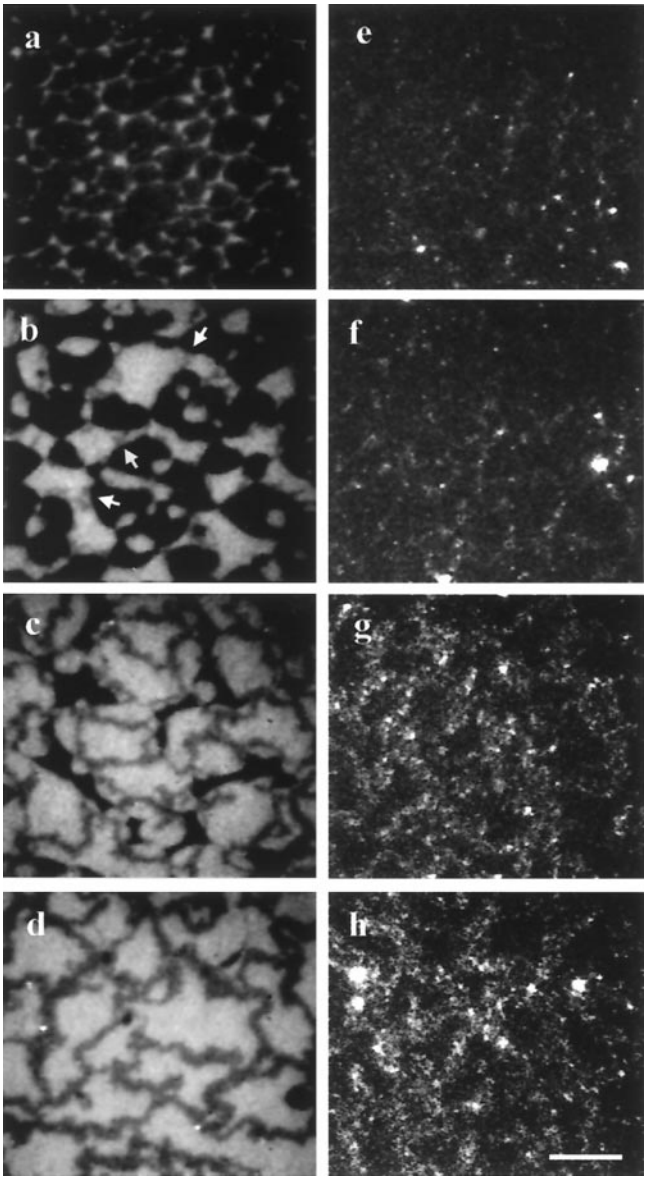

Fig. 4. Fluorescence (*a–d*) and corresponding LSM (*e–h*) images of fibril development during the expansion experiment. (*a* and *e*) The first clear fluorescence is seen at 12 mN/m and 60 Å^2 per DPPC molecule and is accompanied by faint scattering. (*b* and *f*) Upon further expansion (10.2 mN/m, 68 Å^2 per DPPC molecule), gray fibers (see arrows) are observed growing between the LC domains; light scattering is exclusively from the fibrils. (*c* and *g*) As LC domains dissolve (9.7 mN/m, 80 Å^2 per DPPC molecule), the gray networks grow thicker and scattering becomes more intense. (*d* and *h*) At full expansion (8.7 mN/m, 110 Å^2 per DPPC molecule) networks are stable and continue to grow independently. The quenched appearance of the fibers is caused by the TRITC label, which can associate into nonfluorescent dimers (see text). (Scale bar is 20 μm.)

over the time scale of the experiments (8–10 h) and when compressed to high surface pressures ($\pi > 20$ mN/m). They were also observed to undergo thermal motion in the form of lateral bending, suggesting that they are flexible.

To confirm that the assembly of Fn fibrils during monolayer expansion was not an artifact caused by aggregation in solution or surface rheological forces, labeled Fn was adsorbed to the plain air/buffer interface ($t \approx 2$ h) and the interface was expanded as above. In spite of the fact that Fn is partially exposed to a nonpolar environment, there was no evidence of fibril formation. The experiment shown in Fig. 4 was repeated with equimolar concentrations of two other proteins, albumin and fibrinogen. Although fibrinogen was attracted to domain edges as the monolayer was expanded, the protein contracted around shrinking domains rather than becoming stretched between them. Scattering was associated only with large protein aggregates distributed uniformly in the interface (not shown). Similarly, adsorption of albumin did not result in network formation, and the low-intensity light scattering lacked structure. Thus, fibril formation by Fn upon monolayer expansion is not a general characteristic of proteins adsorbed to DPPC monolayers.

Fn in a Fibrillar State. Considerable information on the characteristics of the fibrillar state can be deduced from combined fluorescence and LSM. The sensitivity of the equipment used here was not sufficient to detect scattered light either from the edges of the LC domains embedded in the LE phase of pure DPPC or in the protein-enriched LE phase. Similarly, we did not observe light scattered from the two-dimensional Fn aggregates that formed in the LE phase lipid during static LE/LC coexistence phase experiments (Fig. 2*c*). The fact that the gray fibrils scatter light suggests that they differ considerably in three-dimensional thickness and/or refractive index relative to the surrounding monolayer. The low fluorescence intensity of Fn fibrils (Fig. 4 *b–d*) may be explained by the formation of nonfluorescent rhodamine dimers that arise when neighboring TRITC molecules are in close proximity (3–6 Å) (28–30).

The packing density of Fn in its fibrillar state was further investigated by probing the solvent accessibility of the fluorophores. An ionic fluorescence quencher (KI) was injected into the subphase at 0.3 M concentration after stable fibrils had formed. Fn fluorescence in the subphase was completely quenched, but a small signal remained associated with the fibrils. The greatest remaining fluorescence corresponded to areas exhibiting the most intense light scattering (data not shown). Taken with LSM results, these data indicate that Fn fibrils consist of densely packed proteins that are inaccessible to large ions such as iodide.

Although Fn fibrils appear homogeneous when viewed in fluorescence, they give rise to numerous scattering centers along their length. Because the mature fibrils are at least a few micrometers in diameter, the existence of small scatterers suggests that the outer surface is rough on a nanoscale. One possibility is that Fn aggregates from the LE phase are attracted and adhere to the fibrils. These aggregates would then act as light-scattering sources and possibly as a protein reservoir, allowing rapid thickening of the fibrils as they are pulled (see below). Aggregates would exhibit dimer quenching only after adhesion to a fibril that is being stretched, which would allow rhodamine molecules to align along the fibril and dimerize. This hypothesis is supported by the fact that the bands of scattering centers associated with the partially quenched fibrils consistently cover larger diameters than the fibrils themselves when they are viewed in fluorescence (Fig. 4 *c* and *d* compared with *g* and *h*). This idea may also explain why the fibrils become larger in diameter concomitant to being pulled lengthwise.

To determine whether the monolayer networks were stabilized by disulfide crosslinking similar to Fn in cellular matrices (31), reducing and nonreducing SDS/PAGE was performed. In nonreduced samples, silver staining revealed a band at 450 kDa, as well as another band at the top of the 4% stacking gel that did not enter the resolving gel (data not shown). The 450-kDa band is likely to correspond to bulk and LE phase Fn picked up when the protein was pipetted from the interface. The presence of the high molecular band supports the hypothesis that proteins within the fibrils are tightly associated by disulfide bridges. Reduced samples migrated as a single ≈220-kDa band.

The monolayer expansion speed was critical to the formation

of Fn networks. Expansion rates of 0.1 to 0.2 Å^2 per DPPC molecule per min led to fibril formation, whereas those conducted at speeds between 1 and 2 Å^2 per DPPC molecule per min (a 10-fold increase) did not. By measuring the longest fibril connected by two LC domains in a given frame as a function of time, we were able to determine that the maximal pulling rate in our system was 0.2 μm/min. This rate compares well with the maximum growth rate of 4.7 μm/min found for *Xenopus* blastocele roof cells (32).

Role of DPPC Domains in Fibril Formation. To determine whether the presence of LC domains within the monolayer was required for fibril assembly, Fn was adsorbed to monolayers of POPC. This lipid does not exhibit an LC phase at room temperature because of a single unsaturated bond in one of its two hydrocarbon chains. To closely replicate the expansion under DPPC, TRITC-labeled Fn was injected underneath POPC that had been compressed to 40 mN/m and 55 Å^2 per POPC molecule followed by a 15-h equilibration. During this period, the only changes observed in the interface were slight increases in surface pressure ($\Delta\pi \approx 4$ mN/m) and fluorescence intensity. During the subsequent expansion of the monolayer (0.4 Å^2 per POPC molecule per min), when the barriers were halted for imaging, a rise in π similar to that seen for Fn adsorbed to DPPC (Fig. 3) was observed ($\approx$1 mN/m in a 5-min interval). Coupled with a rapid increase in monolayer fluorescence intensity, this result indicates that a significant amount of protein was able to enter the interface. However, no protein aggregates formed and no significant light scattering was detected. These results along with those shown in Fig. 1 demonstrate that LE phase lipids do not induce Fn network or aggregate formation.

The role of LC domains was further investigated by video imaging of the monolayer expansion experiments in Fig. 4. In these images, newly formed fibrils grew between adjacent LC domains. As the distance between domains increased, the fibrils remained attached at either end and stretched along the central axis. With continued expansion, fibrils grew both in length and in width. When domains melted, fibrils from different sides of former LC domains joined to form a single strand or a junction of several strands. After the LC domains disappeared from the interface, the networks developed an increasing fractal appearance, implying a release of tension. Thus, LC domains appear to serve as anchors and to produce a mechanical force that is sufficiently strong to pull fibrils.

The above results suggest that although LC domains are necessary for the Fn network assembly, they are not sufficient: monolayer expansion is required to initiate fibril growth. Thus, the interaction of Fn with LC domains and the subsequent expansion of the monolayer define the next critical steps in the fibril assembly pathway.

Molecular Mechanism of Fn Fibril Assembly. Our results demonstrate that Fn networks can be formed underneath DPPC lipid monolayers in the absence of membrane receptors. The characteristics of Fn fibrillar structures are that (*i*) they form between LC domains; (*ii*) they give rise to significant light scattering as they grow in length and diameter; and (*iii*) although they appear stretched in the first phases of monolayer expansion, they later assume a fractal appearance, suggesting that they were initially formed under tension and that they are elastic. The presence of condensed DPPC domains and slow expansion of the interfacial film are the critical factors for initiating spontaneous self-assembly of the protein. The molecular model of fibril assembly inferred from our experiments is presented in Fig. 5. We postulate the following sequential steps:

(i) Insertion into the LE phase of the monolayer. When a DPPC monolayer is expanded from the LC phase into the LC/LE phase coexistence, Fn partially inserts into the LE phase (Fig. 5 *Top*).

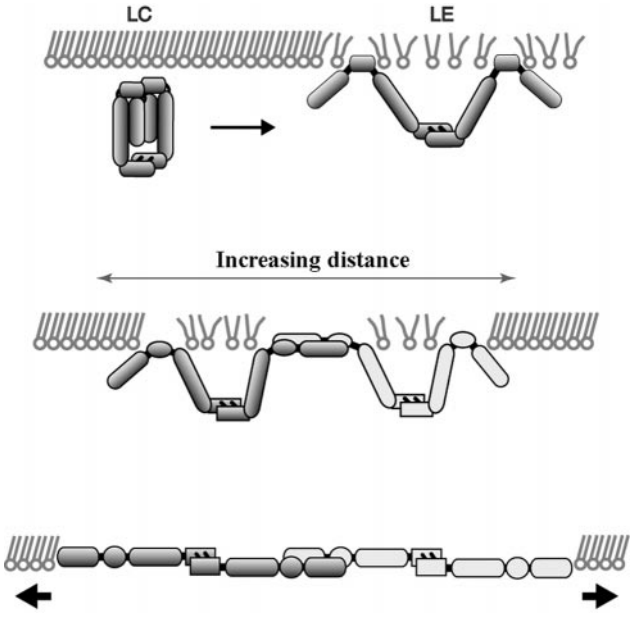

Fig. 5. Schematic of critical events in fibril assembly under DPPC monolayers. Partial insertion of Fn into the LE phase (*Top*) promotes conformational changes in the protein and attraction to domain edges. As the monolayer surface area is increased, long-range repulsive interactions between domains causes them to move apart (*Middle*). If the separation is slow, Fn proteins on neighboring domains initially remain in physical contact, permitting adhesive interactions to develop between them. Mechanical tension caused by domain separation pulls the proteins into an extended conformation, exposing self-assembly sites (*Bottom*).

Fn presumably orients at the interface so that its hydrophobic segments interact with the DPPC acyl chain moiety, resulting in Fn anchoring to condensed lipid domains. A likely candidate is the 14-kDa low-affinity heparin-binding fragment, which includes the III_1 module found to be important for cellular matrix assembly. Using hydrophobic interaction chromatography, Hayashi-Nagai *et al.* (33) found that the 14-kDa fragment had the highest surface hydrophobicity of five thermolysin fragments generated. The more hydrophilic segments (e.g., the 140- to 150-kDa cell binding fragment) would form loops extending into the aqueous subphase.

(ii) Enrichment at the domain boundaries. Attractive interactions between surface adsorbed Fn and LC domains, possibly caused by entropic and/or electrostatic forces (26, 27), lead to the migration of Fn from the LE phase to domain boundaries and result in its enrichment at this location. Furthermore, when the density of Fn in the LE phase exceeds a critical value because of adsorption from solution, aggregation begins (i.e., Fig. 4*c* and the increasing number of light-scattering centers in the LE phase in Fig. 4 *e–h*). A rim of adhesive Fn molecules and aggregates is thus formed around each domain. Presumably, this accumulation of polar oriented Fn molecules enhances the collision rate of Fn self-assembly sites. During the early stages of expansion the interdomain distance is small, which permits the Fn-enriched rims to overlap.

(iii) Pulling of Fn fibrils. Expansion of the monolayer initiates the pulling of Fn into extended fibrils by virtue of an increasing distance between neighboring domain boundaries (Fig. 5 *Middle* and *Bottom*). Mean distances between domain boundaries increase as the LC domains shrink and repulsive interactions drive them apart. The dipole density of the close-packed LC phase is approximately twice that of the LE phase in the absence of proteins (see refs. 24 and 34 and references therein). This typically leads to a quasihexagonal ordering of domains in the

LE/LC phase coexistence of pure lipid monolayers, whereby the relative distances of the domains are maximized.

For the separation of domains to create tensile forces on individual proteins, attractive interactions must exist between Fn and the domain boundaries as well as between adjacent Fn molecules. Experiments in which Fn was adsorbed to the LE/LC phase coexistence region have confirmed that Fn is attracted to LC domain boundaries. The aggregation of Fn in the LE phase, coupled with recent evidence that Fn matrices grown in cell culture are elastic (9), suggests that attractive forces between Fn molecules are sufficient to permit monolayer Fn to be stretched into an extended conformation.

Elongation may occur by increasing interdomain distances combined with the association of additional Fn from the protein-enriched LE phase or the subphase. When the LC domains eventually melt away, fibrils protruding from domain edges are pulled together and intersect, resulting in a two-dimensional fibrillar protein network (Fig. 4*d*).

Comparison to Cell-Mediated Fibril Assembly. The assembly of Fn fibrils under DPPC monolayers displays striking similarities to fibrils assembled on cell surfaces. Like the cell-free networks, cell-mediated matrix assembly is thought to progress through sequential stages. We propose that, although the anchoring mechanism that leads to initiation of fibrillogenesis may be different, the pathway by which surface-bound Fn is assembled into fibrils is similar.

It has been hypothesized that fibril formation on cellular surfaces begins with a "surface activation" step in which binding to cell surfaces by means of integrins or other surface proteins induces conformational changes in the protein that expose Fn–Fn binding sites (7, 35, 36). In our system, exposure of these sites could be facilitated by nonspecific binding of Fn to the LE phase of DPPC.

A growing body of evidence suggests that mechanical tension is critical for initiation of cell-mediated matrix assembly. Fibril formation is frequently observed at sites of tension such as at the lateral and retracting edges of cells (37) and at focal adhesions (38). Cells that are unable to generate contractile forces are also incapable of constructing a Fn matrix (8, 39). In addition, the mechanical stretching of immobilized Fn increases the binding of soluble Fn and the L8 monoclonal antibody, whose epitope is important for matrix assembly, suggesting that stretched Fn is capable of nucleating self-assembly (40). In the lipid monolayer system, enrichment of Fn at domain edges and mechanical pulling during expansion could presumably expose cryptic Fn–Fn binding sites.

In conclusion, we have demonstrated that fibrillar networks of Fn can be generated in noncellular environments and have analyzed the pathway by which they form. As in cell-mediated assembly, mechanical tension is crucial for initiating fibril formation. Striking similarities were found between the characteristic of Fn fibrils assembled underneath DPPC monolayers and those formed on cellular surfaces, including their sequential assembly. The spontaneous assembly of Fn fibrils underneath DPPC monolayers could now serve as a well-controlled model system for detailed studies of the assembly pathway and how it is affected by external factors. Parameters that can be examined include the effect of solution conditions and surface composition, and the presence of other Fn-binding proteins such as heparin and collagen. The significance of selected Fn modules may be directly studied by using recombinant proteins without concern for potential alterations in cell signaling or metabolism.

We gratefully acknowledge fruitful discussions and editorial comments by André Krammer, François Baneyx, and John Glomset. This work was funded through National Institutes of Health First Award GM 49063 (V.V.) and a National Science Foundation Graduate Fellowship (G.B.).

1. Hynes, R. O. (1990) *Fibronectins* (Springer, New York).
2. McKeown-Longo, P. J. & Mosher, D. F. (1985) *J. Cell Biol.* **100,** 364–374.
3. Quade, B. J. & McDonald, J. A. (1988) *J. Biol. Chem.* **263,** 19602–19609.
4. Hocking, D. C., Smith, R. K. & McKeown-Longo, P. L. (1996) *J. Cell Biol.* **133,** 431–444.
5. Aguirre, K. M., McCormick, R. J. & Schwarzbauer, J. E. (1994) *J. Biol. Chem.* **269,** 27863–27868.
6. Morla, A. & Ruoslahti, E. (1992) *J. Cell Biol.* **118,** 421–429.
7. Sechler, J. L., Corbett, S. A. & Schwarzbauer, J. E. (1997) *Mol. Biol. Cell* **8,** 2563–2573.
8. Halliday, N. L. & Tomasek, J. J. (1995) *Exp. Cell Res.* **217,** 109–117.
9. Ohashi, T., Kiehart, D. P. & Erickson, H. P. (1999) *Proc. Natl. Acad. Sci. USA* **96,** 2153–2158.
10. Peters, D. M., Portz, L. M., Fullenwider, J. & Mosher, D. F. (1990) *J. Cell Biol.* **111,** 249–256.
11. Dzamba, B. J. & Peters, D. M. (1991) *J. Cell Sci.* **100,** 605–612.
12. Sottile, J. & Mosher, D. F. (1997) *Biochem. J.* **323,** 51–60.
13. Mosher, D. & Johnson, R. B. (1983) *J. Biol. Chem.* **258,** 6595–6601.
14. Williams, E. C., Janmey, P. A., Johnson, R. B. & Mosher, D. F. (1983) *J. Biol. Chem.* **258,** 5911–5914.
15. Sakai, K., Fujii, T. & Hayashi, T. (1994) *J. Biochem. (Tokyo)* **115,** 415–421.
16. Morla, A., Zhang, Z. & Ruoslahti, E. (1994) *Nature (London)* **367,** 193–196.
17. Brown, R. A., Blunn, G. W. & Ejim, O. S. (1994) *Biomaterials* **15,** 457–464.
18. Ejim, O. S., Blunn, G. W. & Brown, R. A. (1993) *Biomaterials* **14,** 743–748.
19. Haugland, R. P. (1996) *Handbook of Fluorescent Probes and Research Chemicals* (Molecular Probes, Eugene, OR).
20. Adamson, A. W. & Gast, A. P. (1997) *Physical Chemistry of Surfaces* (Wiley, New York).
21. Grainger, D. W., Reichert, A., Ringsdorf, H. & Salesse, C. (1989) *FEBS Lett.* **152,** 73–82.
22. Wessel, D. & Flugge, U. I. (1984) *Anal. Biochem.* **138,** 141–143.
23. Haas, H. & Möhwald, H. (1989) *Thin Solid Films* **180,** 101–110.
24. Möhwald, H. (1990) *Annu. Rev. Phys. Chem.* **41,** 441–476.
25. Diederich, A., Sponer, C., Pum, D., Sleytr, U. B. & Lösche, M. (1996) *Colloids Surf. B* **6,** 335–346.
26. Nassoy, P., Birch, W. R., Andelman, D. & Rondelez, F. (1996) *Phys. Rev. Lett.* **76,** 455–458.
27. Netz, R. R., Andelman, D. & Orland, H. (1996) *J. Phys. II* **6,** 1023–1047.
28. Davydov, A. S. (1962) *Theory of Molecular Excitons* (McGraw-Hill, New York).
29. Packard, B. Z., Toptygin, D. D., Komoriya, A. & Brand, L. (1996) *Proc. Natl. Acad. Sci. USA* **93,** 11640–11645.
30. Packard, B. Z., Komoriya, A., Toptygin, D. D. & Brand, L. (1997) *J. Phys. Chem. B* **101,** 5070–5074.
31. McKeown-Longo, P. J. & Mosher, D. F. (1983) *J. Cell Biol.* **97,** 466–472.
32. Winklbauer, R. & Stoltz, C. (1995) *J. Cell Sci.* **108,** 1575–1586.
33. Hayashi-Nagai, A., Kitagaki-Ogawa, H., Matsumoto, I., Hayashi, M. & Seno, N. (1991) *J. Biochem. (Tokyo)* **109,** 83–88.
34. McConnell, H. M. & De Koker, R. (1995) *Langmuir* **12,** 4891–4904.
35. Barry, E. L. & Mosher, D. F. (1988) *J. Biol. Chem.* **263,** 10464–10469.
36. Limper, A. H., Quade, B. J., LaChance, R. M., Birkenmeier, T. M., Rangwala, T. S. & McDonald, J. A. (1991) *J. Biol. Chem.* **266,** 9697–9702.
37. Peters, D. M. & Mosher, D. F. (1987) *J. Cell Biol.* **104,** 121–130.
38. Christopher, R. A., Kowalczyk, A. P. & McKeown-Longo, P. J. (1997) *J. Cell Sci.* **110,** 569–581.
39. Zhang, Q., Magnusson, M. K. & Mosher, D. F. (1997) *Mol. Biol. Cell* **8,** 1415–1425.
40. Zhong, C., Chrzanowska-Wodnicka, M., Brown, J., Shaub, A., Belkin, A. M. & Burridge, K. (1998) *J. Cell Biol.* **141,** 539–551.
41. Weis, R. M. & McConnell, H. M. (1984) *Nature (London)* **310,** 47–49.
42. Frey, W., Schief, W. R., Jr., & Vogel, V. (1996) *Langmuir* **12,** 1312–1320.
43. Schief, W. R., Jr., Dennis, S. R., Frey, W. & Vogel, V. (1999) *Colloids Surf. A*, in press.